Observation of iron spin-states using tabletop x-ray emission spectroscopy and microcalorimeter sensors

2016 J. Phys. B: At. Mol. Opt. Phys. 49 024003

(http://iopscience.iop.org/0953-4075/49/2/024003)

IOP Publishing Journal of Physics B: Atomic, Molecular and Optical Physics
J. Phys. B: At. Mol. Opt. Phys. **49** (2016) 024003 (7pp) doi:10.1088/0953-4075/49/2/024003

Observation of iron spin-states using tabletop x-ray emission spectroscopy and microcalorimeter sensors

Y I Joe[1], G C O'Neil[1], L Miaja-Avila[1], J W Fowler[1], R Jimenez[1,2], K L Silverman[1], D S Swetz[1] and J N Ullom[1]

[1] National Institute of Standards and Technology, 325 Broadway Boulder, CO 80305–3337, USA
[2] JILA, University of Colorado Boulder, 440 UCB, Boulder, CO 80309, USA

E-mail: joel.ullom@nist.gov

Received 1 June 2015, revised 14 October 2015
Accepted for publication 3 November 2015
Published 22 December 2015

Abstract

X-ray emission spectroscopy (XES) is a powerful probe of the electronic and chemical state of elemental species embedded within complex compounds. X-ray sensors that combine high resolving power and high collecting efficiency are desirable for photon-starved XES experiments such as measurements of dilute, gaseous, and radiation-sensitive samples, time-resolved measurements, and in-laboratory XES. To assess whether arrays of cryogenic microcalorimeters will be useful in photon-starved XES scenarios, we demonstrate that these emerging energy-dispersive sensors can detect the spin-state of 3d electrons of iron in two different compounds, Fe_2O_3 and FeS_2. The measurements were conducted with a picosecond pulsed laser-driven plasma as the exciting x-ray source. The use of this tabletop source suggests that time-resolved in-laboratory XES will be possible in the future. We also present simulations of Kα and Kβ spectra that reveal the spin-state sensitivity of different combinations of sensor resolution and accumulated counts. These simulations predict that our current experimental apparatus can perform time-resolved XES measurements on some samples with a measurement time of a few 10 s of hours per time delay.

Keywords: x-ray emission spectroscopy, transition edge sensor, ultrafast

(Some figures may appear in colour only in the online journal)

1. Introduction

In recent years, x-ray emission spectroscopy (XES) has emerged as an important technique for the study of chemically active elemental species within larger molecules or complexes. In XES, an exciting x-ray flux is used to produce core-hole vacancies that are filled by the relaxation of valence or other core electrons with concomitant x-ray fluorescence. XES provides information on the charge and spin state of the absorbing atomic species as well as on its ligand environment [1, 2]. Because the information in XES is contained in fine structure within an x-ray-fluorescence feature, excellent spectral resolving-power is required. At x-ray energies below 2 keV, gratings are the preferred analyzer and at higher energies, crystal analyzers are used. Bright exciting x-ray beams are often used to compensate for the limited collection efficiency of these wavelength-dispersive technologies. Recent advances in the collection efficiency and energy resolution of crystal analyzers have increased the feasibility of XES in laboratory settings when excitation fluxes are usually lower [3, 4]. The use of cryogenic microcalorimeters has recently been proposed for XES and their ability to provide chemical specificity was demonstrated [5]. The primary motivating attraction of these energy-dispersive detectors is a large potential increase in photon-collection efficiency. Deployed microcalorimeter spectrometers with 240 sensing elements already provide a hundred-fold efficiency improvement at the nitrogen and oxygen Kα lines over some high-efficiency gratings. Further, large improvements in the collecting efficiency and photon throughput are anticipated

for these microcalorimeter arrays [5, 6]. Increased collection efficiency is desirable for a range of scenarios including studies of dilute, gaseous, and radiation-sensitive samples, time-resolved measurements, and laboratory XES where the exciting x-ray fluxes available are much less intense than at large facilities such as synchrotron and free electron laser. As part of assessing the utility of cryogenic microcalorimeters for XES, it is important to determine whether the resolving power of this technology permits the detection of scientifically relevant XES features on practical timescales. While the resolving power of cryogenic microcalorimeters is generally lower than that of gratings and crystals, Uhlig *et al* [5] compared present and potential energy-resolution values to line broadening due to finite core hole lifetimes. Over wide energy ranges, the resolution of cryogenic microcalorimeters was shown to be less than or comparable to core hole broadening, a favorable condition for XES.

Here, we focus on demonstrating and assessing the suitability of cryogenic microcalorimeters for a specific XES measurement: the determination of the spin-state of molecular iron. Iron is representative of the 3d-transition metals found in many naturally occurring compounds. We use an array of superconducting transition-edge sensors (TESs), currently the most mature cryogenic-microcalorimeter technology, to show that both the iron Kα and Kβ emission features can be used to distinguish between low-spin (LS) and high-spin (HS) iron compounds. These measurements were performed with a picosecond pulsed-laser-driven plasma as the exciting x-ray source. While the results presented here do not show time-resolved dynamics, the use of this tabletop source for excitation demonstrates the potential of cryogenic microcalorimeter arrays to perform time-resolved, in-laboratory XES. In addition, we present simulations of Kα and Kβ spectra from LS and HS compounds at different sensor energy resolutions and numbers of accumulated counts. These simulations show the potential of cryogenic microcalorimeters to detect intermediate spin-states under a range of experimental conditions.

Molecular systems with switchable electronic states are desirable for complex functionalities. For example, transition-metal complexes that undergo long-lived charge separation are candidates for solar-energy harvesting. Metal-to-ligand-charge-transfer (MLCT) states in these complexes can be induced by excitation at visible wavelengths. The formation of a MLCT is often accompanied by spin cross-over meaning a change in the spin-state of the 3d orbital shell of the metal center [7]. A spin change can occur in materials separately from MLCT, for example as a result of changes in temperature or pressure [8, 9]. XES is an effective probe of the spin state because the local magnetic moment of the 3d shell perturbs the 3p orbitals and hence the shape of the Kβ x-ray line produced by 3p-to-1s transitions [10]. The Kα x-ray complex produced by the 2p-to-1s transitions is also affected. An XES measurement combined with reference data can be used to make quantitative determinations of spin-state, even under challenging dynamical conditions [11, 12]. Figure 1 shows an energy-level schematic of Fe(II) for spin zero and spin two. Other spin values are possible depending on the material and conditions. The ability to determine the spin state during chemical or photoreactions is of great interest because it can be used to identify reaction products as well as pathways and intermediate states.

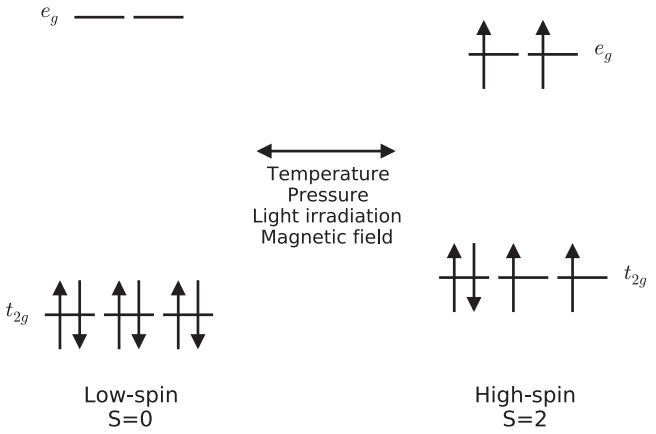

Figure 1. Energy level schematic showing low-spin and high-spin states of the 3d orbital shell of Fe(II). Electrons are denoted by arrows that indicate spin direction.

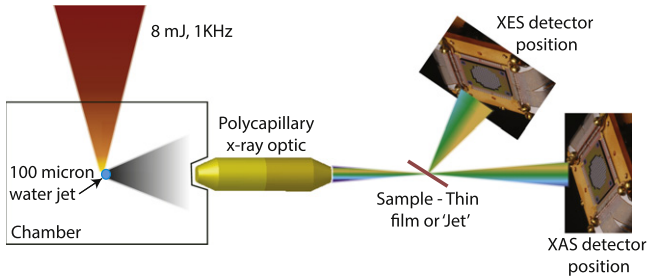

Figure 2. Schematic of the plasma source/cryogenic microcalorimeter x-ray laboratory apparatus. Femtosecond laser pulses are focused onto the edge of a water jet to produce a plasma and Bremsstrahlung x-rays. The x-rays are focused via a polycapillary optic onto the sample of interest. For absorption spectroscopy, the transmitted x-rays are measured with the microcalorimeter array. For emission spectroscopy, the microcalorimeter array is moved out of the path of the exciting beam so that the observed x-ray flux is dominated by sample fluorescence. Although not shown here, the system is capable of optical pump/x-ray probe measurements by splitting the laser beam and focusing part of it onto the sample prior to the arrival of the x-ray probe pulse.

2. Experiment setup

The XES measurements presented here were acquired with a laboratory x-ray source capable of producing picosecond x-ray pulses. A schematic of the experimental setup is shown in figure 2 and a full description of the system is given in [18]. The source makes use of a commercial pulsed Ti:Sapphire laser with a repetition rate of 1 kHz. The laser produces 800 nm photons in intense, 40 fs pulses. The pulsed-laser beam is tightly focused onto the edge of a cylindrical water jet enclosed in a chamber held at a weak vacuum of approximately 9 Torr. The high-intensity laser pulse creates a plasma and thus generates a broadband Bremsstrahlung x-ray

spectrum from approximately 1 to 14 keV. The x-ray flux at the sample position depends on a range of experimental conditions. For the measurements presented here, the flux was approximately 4×10^6 photons per second with a spectral distribution peaked at 7 keV. Because the plasma source emits x-rays into 4π solid angle, a polycapillary x-ray optic is used to collect and refocus the x-rays onto a 75 μm diameter circular spot. While the intrinsic duration of the x-ray pulses is short, the optic introduces an estimated temporal broadening of 1.6 ps. The sample of interest is placed at the output focus of the optic which is located 25 mm from its exit face and 140 mm from the water jet.

This x-ray source is designed for 'optical pump—x-ray probe' measurements. For pump-probe measurements, each laser pulse is split prior to interaction with the water jet. The 'pump' beam is focused onto the sample after passing through a delay stage, while the 'probe' beam is focused onto the water jet. The sample is thus probed with the pulsed x-rays at controlled time delays after the optical pump. The emission measurements presented here did not make use of an optical pump and thus could have been obtained with a more conventional excitation source such as an x-ray tube. However, use of the laser driven plasma source is an important step towards demonstrating the feasibility of dynamic emission measurements of materials that undergo optical excitations on picosecond and longer timescales utilizing tabletop laboratory instrumentation. More specifically, these measurements show that the combination of a pulsed excitation source and a microcalorimeter array can produce x-ray spectra with sufficient energy resolution and statistics to reveal LS and HS behavior.

The low collecting efficiency of wavelength-dispersive spectrometers is poorly matched to the modest x-ray fluorescence excited by our laser driven plasma source. Instead, we collect and measure the fluorescence with an array of superconducting TES detectors. TES detectors are microcalorimeters that measure the energy of individual photons through the temperature change of a superconducting thin-film. When a photon is absorbed, the film temperature increases by an amount proportional to the photon energy. The film is voltage-biased into the resistive transition so that small changes in its temperature result in large changes in its resistance. The resulting resistance increase results in a current pulse, which is read out via an inductively coupled SQUID ammeter. The height of this current pulse is a sensitive measure of photon energy. Descriptions of TES spectrometers and their readout electronics are given in [13] and [14]. In our experiment, we employed an array of 240 TES detectors. Each detector consists of a 300 nm thick MoCu bilayer with a 4 μm thick Bi x-ray absorber patterned on top of the device. After collimation, each detector has an active area of $320 \times 305\ \mu m^2$. The energy resolution of a TES detector is determined by thermodynamic power fluctuations between the detector and the local heat bath, as well as Johnson noise in the resistive sensing element [15]. Ultrahigh resolving powers are achieved by operation of the sensors at cryogenic temperatures near 0.1 K to minimize thermodynamic-fluctuation noise. To maintain large solid-angle coverage, the sensors were placed approximately 50 mm from the sample, so that the array occupied a solid angle near 10^{-2} sr. At the energies of interest near 7 keV, the Bi absorbers have greater than 70% quantum efficiency and the combined loss due to air and windows is less than 5%.

The pulsed laser/microcalorimeter array apparatus can be configured to measure either x-ray emission or x-ray absorption spectra. For x-ray absorption, the spectrometer is placed in-line with the x-ray optic and sample. X-ray absorption measurements from the same apparatus are shown in [18]. To measure x-ray emission, the spectrometer is rotated roughly 10° out of the path of the probing x-ray beam so that the observed x-ray flux is dominated by sample fluorescence (see figure 2). Here, we present the first x-ray emission measurements from our apparatus.

3. Measurements

The ability to distinguish HS from LS iron compounds is a good test of whether cryogenic microcalorimeters can perform XES. Using the apparatus described above, we measured emission spectra from two compounds, FeS_2 and Fe_2O_3, that contain iron in different spin states. The sample materials, purchased from a commercial vendor, were ground with a mortar and pestle for many minutes. The typical particle size after grinding was estimated to be 5–10 μm based on inspection with an optical microscope. The ground samples were then spread onto the sticky side of a piece of 25 μm thick polyimide tape with a rubber-tipped spatula. The tape was folded over and the outside edge was sealed with additional tape. The masses per unit area of the FeS_2 and Fe_2O_3 samples were 4 and 3.3 mg cm^{-2} respectively. The samples were excited with broadband x-rays produced by the laser-driven plasma source. The measured Kα and Kβ emission line complexes of these two compounds are shown in figure 3. The broadband energy response of microcalorimeters allows the Kα and Kβ lines to be measured simultaneously. The integration times for the FeS_2 and Fe_2O_3 spectra were 248 and 190 min, respectively. This acquisition time was determined by the intensity of the exciting x-ray flux. The sensors were operating at less than one tenth of their count rate capability. Hence, this spectrometer could acquire the same spectra in 25 and 19 min given a 10×brighter exciting source such as those described by Reich *et al* [19] and Zamponi *et al* [20]. The energy resolution of the spectrometer in this measurement was 5.5 eV FWHM. While this resolution is more than twenty times better than the fundamental limit of silicon-based energy-dispersive detectors, it is far from the fundamental limit of microcalorimeter technology. At 8 keV, single microcalorimeter sensors have already demonstrated energy resolution values of 2.0 eV [21], and 2.5 eV energy resolution has been demonstrated in a 30 pixel array at 6 keV [26].

The 3d electrons in the Fe atoms in Fe_2O_3 and FeS_2 are known to occupy HS and LS states, respectively. These spin states can be confirmed from the data of figure 3. The Kα spectra show a statistically significant change in the ratio of

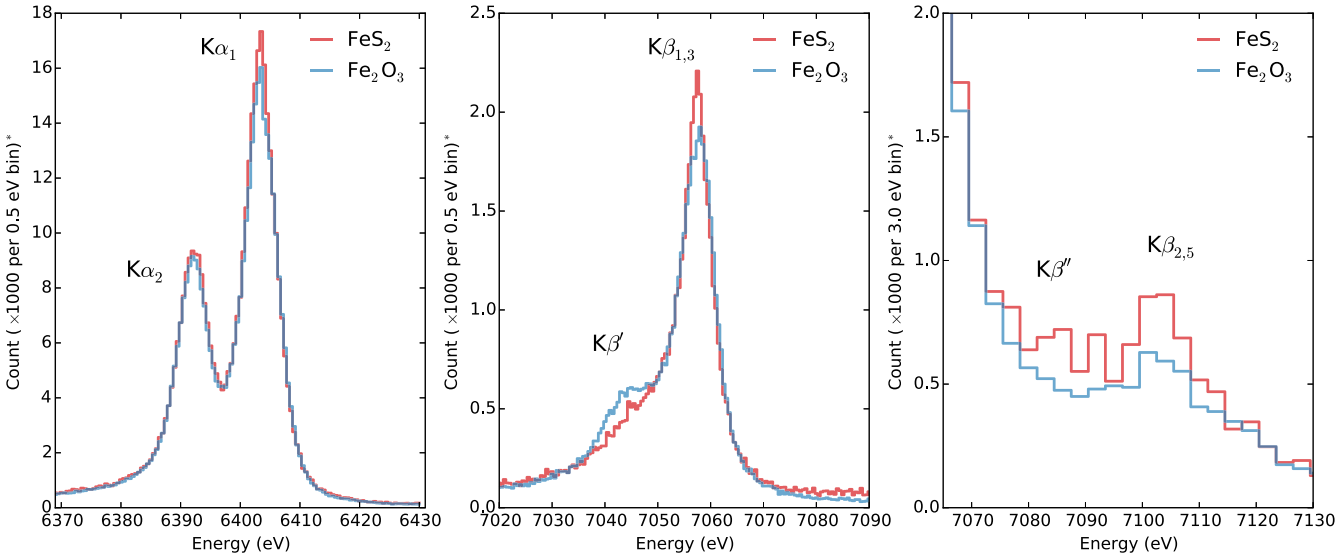

Figure 3. XES data from Fe_2O_3 and FeS_2 acquired using a laser driven x-ray plasma source to produce core hole vacancies and an energy dispersive cryogenic microcalorimeter spectrometer to measure the resulting x-ray fluorescence. The Fe 3d electrons of Fe_2O_3 and FeS_2 occupy HS and LS states respectively. * The vertical scale is for Fe_2O_3 spectra, and FeS_2 spectra are scaled as described in the text.

the Kα_1 and Kα_2 intensities with respect to achievable SNR. The Kβ spectrum of HS Fe_2O_3 clearly shows a satellite Kβ' peak below the main K$\beta_{1,3}$ feature. Further, the high energy K$\beta_{2,5}$ feature is enhanced in the LS material FeS_2. All these signatures are in excellent agreement with published spectra of HS and LS iron compounds acquired with a crystal spectrometer [8]. The Kα spectra in figure 3 were normalized to the Kα_2 peak amplitude. The main K$\beta_{1,3}$ spectra were normalized to the spectral area and the K$\beta_{2,5}$ spectra shared this normalization.

XES spectra can reveal more than the spin-state of a material. The centroid of the K$\beta_{2,5}$ feature is correlated with the oxidation state of the metal. The centroid and intensity of a faint Kβ'' feature can be used to identify the bond lengths and type of the elements bonded to the metal center [22]. While the spectra shown in figure 3 are not of sufficient quality for this level of analysis, reasonable improvements in energy resolution and counting statistics may provide this information in the future.

4. Simulation

In the static XES measurements presented in the previous section, the spin state of the 3d electrons is either entirely HS or entirely LS. However, in dynamic measurements, the SNR is lower because the material under study contains an evolving mix of LS and HS states in response to the optical pump. The XES spectra of the sample will therefore contain contributions from high, low, and sometimes intermediate spin states of Fe atoms. To assess the ability of cryogenic microcalorimeters to detect these complex spin-state variations, we have performed numerical simulations based on published reference data. It is common to describe an evolving material in terms of an excitation fraction, meaning the fraction of atoms that have transitioned from one state to another. Experimentally realizable excitation fractions in response to an optical-pump pulse depend on many factors including the concentration of the sample, the wavelength, duration, and fluence of the pump; hence a simple characterization would not be possible. However, for intense sub-picosecond pulses, spin-state excitation fractions of 20% are realistic [16]. As a result, we have simulated the accuracy with which excitation fractions between 0% and 20% can be determined with XES. The integral of the absolute value of the difference (IAD) between two Kβ spectra is a widely used indicator of the local spin state of the 3d orbital in Fe atoms [8, 10]. In order to assess the feasibility of detecting 3d local spin dynamics with a time-resolved laboratory XES apparatus, Fe Kβ spectra of pumped and unpumped samples were simulated at different excitation fractions, numbers of Kβ emission photons, and detector energy resolutions. At a given excitation fraction, the underlying Fe Kβ spectral distribution is constructed as a linear combination of the LS and HS spectra reported by Lin *et al* [17]. After the unpumped and pumped spectra were convolved with a detector-response function, the effects of photon statistics were incorporated by setting the overall number of counts in the spectra and assuming Poisson fluctuations in the number of photons in each energy bin. Subsequently, the IAD value was calculated from the two histograms that describe the pumped and unpumped spectra. We performed 100 independent simulations at each combination of parameters in order to determine the mean IAD value and its statistical error. Figure 4 shows the simulated IAD values for four different combinations of parameters. As the number of Kβ x-ray emission photons increases and the energy resolution of the detectors improves, the IAD yields a more accurate spin state estimation and the detection threshold of changes in the excitation fraction decreases. The number of emission photons has an especially significant impact on spin-state determination. Taking figure 4(c) as an example (10^6 Kβ photons and 6 eV resolution), the IAD

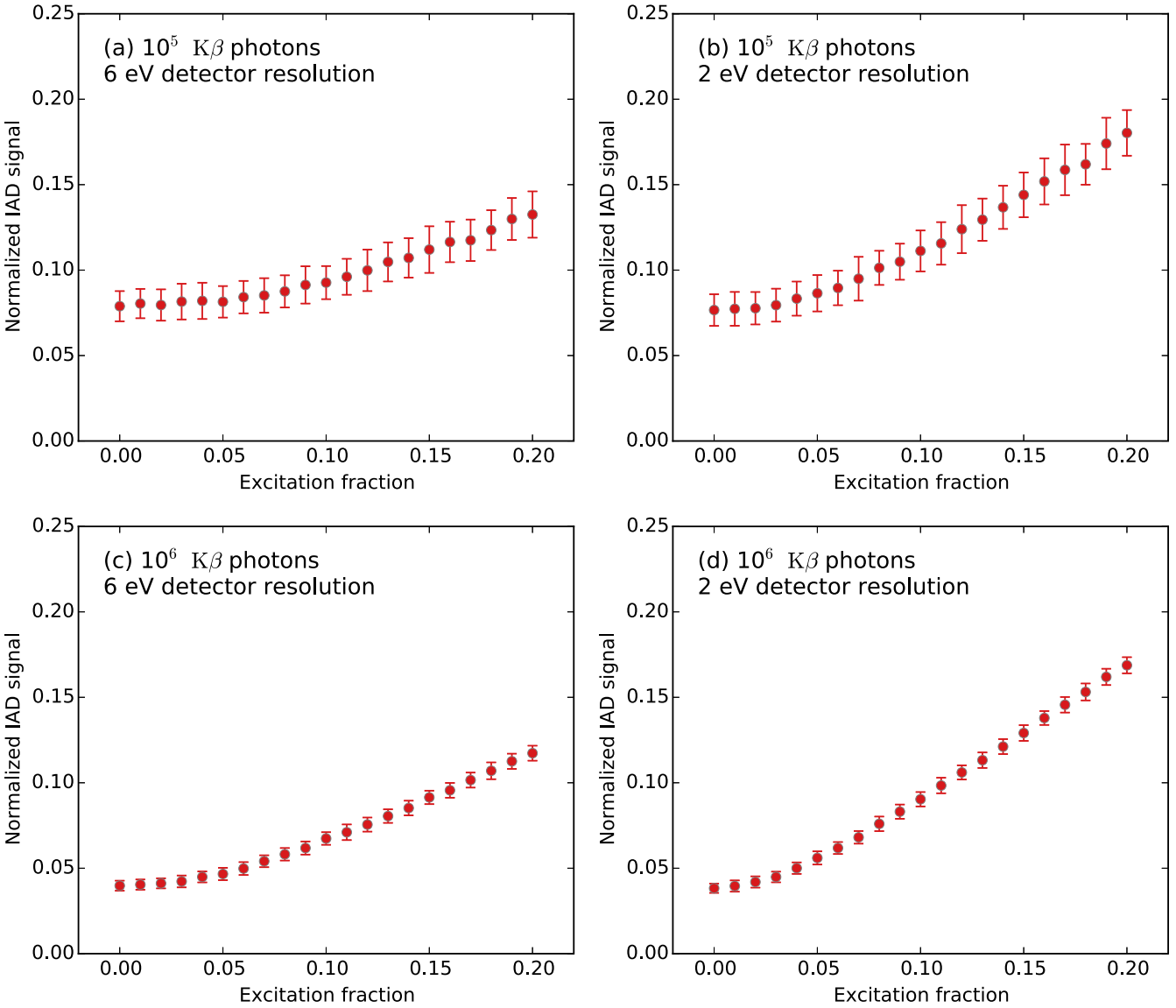

Figure 4. Simulated IAD value at different excitation fractions. (a) 10^5 Kβ photons and 6 eV detector resolution. (b) 10^5 Kβ photons and 2 eV detector resolution. (c) 10^6 Kβ photons and 6 eV detector resolution. (d) 10^6 Kβ photons and 2 eV detector resolution. Error bars indicate $\pm$ one standard deviation.

values for excitation fractions that differ by 2% (i.e. 18% and 20%) are separated by about two standard deviations. These results strongly suggest that accurate spin-state measurements are possible given sufficient numbers of measured photons, even with no further improvement in energy resolution.

The Fe Kα line complex also exhibits spin-state-dependent features, which include the Kα_1/Kα_2 intensity ratio, the peak width of Kα_1, and the energy separation between Kα_1 and Kα_2 [8]. Even though Kα spectra are not as widely used for spin-state determination as Kβ spectra, the intensity of the Kα complex is approximately 10 times stronger so its future use is attractive. We therefore performed simulations of pumped and unpumped Fe Kα spectra in order to estimate the excitation fraction detection limits that can be achieved from this spectral region. Simulated Kα emission spectra were constructed from linear combinations of the LS ($S = 0$) and HS ($S = 2$) Kα emission lines reported by Vankó *et al* [8]. There is not an accepted metric for the comparison of Kα spectra analogous to the IAD developed for the Kβ line. To assess Kα spectra, we propose a slightly modified excitation fraction indicator:

$$\text{Indicator}(s) = \int \mathrm{d}E\ (s(E) - l(E))(h(E) - l(E)),$$

where $h(E)$ and $l(E)$ are reference spectra of HS and LS states and $s(E)$ is a spectrum of mixed state. Figure 5 shows the simulated indicator values and error bars for different excitation fractions assuming 10^6 Kα photons and 6 eV resolution. Excitation fractions that differ by 2% (i.e. 18% and 20%) are separated by slightly less than two standard deviations.

The results of figure 5 suggests that Kα spectra can give more accurate excitation-fraction measurements in the same integration time. For the same detector resolution and the same integration time, the Kα features yield excitation

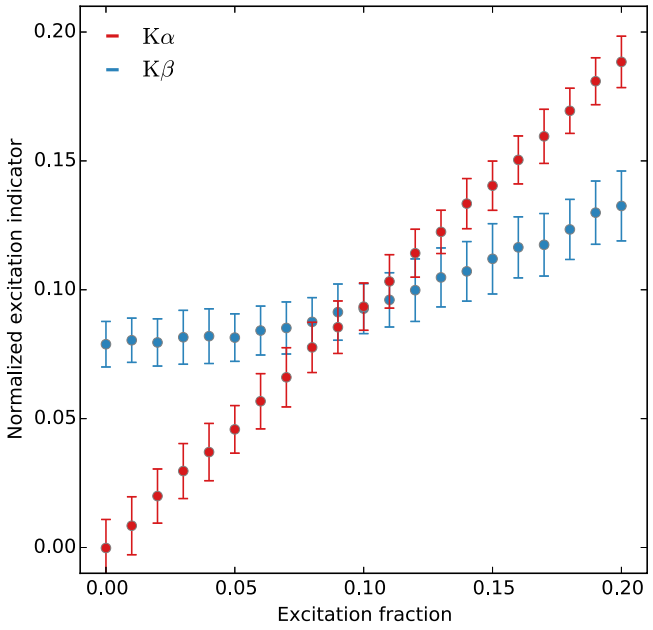

Figure 5. Kα excitation fraction indicator calculated for excitation fractions between 0% and 20%. The simulations assume 10^6 Kα photons and 6 eV detector resolution. Simulated IAD values for 10^5 Kβ photons and 6 eV detector resolution are reproduced for comparison. Error bars indicate ± one standard deviation.

fraction indicators that provide about 1σ of separation per 1% absolute excitation difference. By contrast, Kβ features yield only about $\sigma/3$ of separation per 1% absolute excitation difference. Experimental studies are warranted to explore whether this idea can be realized in practice.

It is valuable to estimate the integration times required to accumulate spectra with 10^6 Kα photons. (The same spectra will also include roughly 10^5 Kβ photons because of the broadband response of microcalorimeter arrays.) The 248 and 190 min of data acquisition for FeS_2 and Fe_2O_3 powders described in section 3 provide useful scaling points. Samples for dynamic pump-probe measurements must satisfy a range of constraints. In particular, due to the shorter interaction lengths in Fe compounds for optical photons than x-rays, the Fe concentrations for pump-probe measurements must be much lower than in the solid samples of section 3 if reasonable optical excitation fractions are to be achieved. Two representative compounds for pump-probe measurements are ferrioxalate [23, 24] and iron tris-bipyridine [7, 11, 12] in aqueous solutions. For sample geometries and concentrations compatible with excitation fractions of 20%, we estimate that the fluorescence x-ray production rates in ferrioxalate and iron tris-bipyridine will be about 2 and 10 times smaller, respectively, than from the solid powders of section 3. With our current experimental set up, the predicted integration time to obtain 10^6 Kα x-rays is 16 hr for ferrioxalate and 80 hr for iron tris-bipyridine. Stable operation for 16 hr is already routine in our apparatus and 80 hr of integration is realistic.

Substantially shorter integration times are anticipated in the future based on multiple reasonable improvements. As noted earlier, laser-driven plasma sources that are brighter than the one used here already exist and could produce a 10× reduction in our count times [19, 20]. Microcalorimeter arrays of several thousand elements instead of 240 are under development and improvements in readout technology [25] are anticipated to allow substantially faster count rates per pixel. Further, the distance between the sample and spectrometer could be reduced by a factor of two. These improvements have the potential to provide at least an additional 10× reduction in count times.

5. Conclusion

We have demonstrated that XES with arrays of cryogenic microcalorimeters can determine the spin-state of 3d electrons in iron compounds, even with sensors whose resolution (5.5 eV) for iron K x-rays is appreciably worse than the best examples of this technology (slightly better than 2 eV). This result and the high collecting efficiency of cryogenic microcalorimeters highlights their attraction for XES in photon-starved scenarios.

The use of a tabletop plasma source as the source of the exciting x-rays strongly suggests that in-laboratory, time-resolved XES measurements of spin-state will be possible in the future. This conclusion is supported by sensitivity simulations that include the impact of excitation fractions substantially below unity. The same simulations predict that iron spin-states can be determined with considerable precision from both Kα and Kβ spectral features and that the same level of spin-state sensitivity can be obtained from the Kα line complex as from the more commonly used Kβ feature but with shorter integration times.

Acknowledgments

We gratefully acknowledge financial support from the NIST Innovations in Measurement Science program and from the DOE Office of Basic Energy Sciences.

References

[1] de Groot F 2001 High-resolution x-ray emission and x-ray absorption spectroscopy *Chem. Rev.* **101** 1779
[2] Glatzel P and Bergmann U 2005 *Coord. Chem. Rev.* **249** 65
[3] Seidler G T *et al* 2014 A laboratory-based hard x-ray monochromater for high-resolution x-ray emission spectroscopy and x-ray absorption edge structure measurements *Rev. Sci. Instrum.* **85** 113906
[4] Anklamm L *et al* 2014 A novel von Hamos spectrometer for efficient x-ray emission spectroscopy in the laboratory *Rev. Sci. Instrum.* **85** 053110
[5] Uhlig J *et al* 2015 High-resolution x-ray emission spectroscopy with transition-edge sensors present performance and future potential *J. Synchrotron Radiat.* **22** 766
[6] Fuchs O *et al* 2009 High-resolution, high-transmission soft x-ray spectrometer for the study of biological samples *Rev. Sci. Instrum.* **80** 063103

[7] Bressler Ch *et al* 2009 Femtosecond XANES study of the light-induced spin crossover dynamics in an Iron(II) complex *Science* **323** 5913
[8] Vankó G *et al* 2006 Probing the 3d spin momentum with x-ray emission spectroscopy: the case of molecular-spin transitions *J. Phys. Chem.* B **110** 11647
[9] Rueff J P *et al* 1999 Pressure-induced high-spin to low-spin transition in FeS evidenced by x-ray emission spectroscopy *Phys. Rev. Lett.* **82** 3284
[10] Gretarsson H *et al* 2011 Revealing the dual nature of magnetism in iron pnictides and iron chalcogenides using x-ray emission spectroscopy *Phys. Rev.* B **84** 100509
[11] Vankó G *et al* 2010 Picosecond time-resolved x-ray emission spectroscopy *Angew. Chem., Int. Ed. Engl.* **49** 5910
[12] Zhang W *et al* 2014 Tracking excited-state charge and spin dynamics in iron coordination complexes *Nature* **509** 7500
[13] Bennett D A *et al* 2012 A high resolution gamma-ray spectrometer based on superconducting microcalorimeters *Rev. Sci. Instrum.* **93** 093113
[14] Ullom J N *et al* 2014 Transition-edge sensor microcalorimeters for x-ray beamline *Synchrotron Radiat. News* **27** 24
[15] Irwin K D and Hilton G C 2005 Transition-edge sensors *Cryog. Part. Detect.* **99** 63
[16] Gawelda W 2006 Time-resolved x-ray absorption spectroscopy of transition metal complex *PhD thesis* École polytechnique fédérale de Lausanne
[17] Lin J *et al* 2007 Spin transition zone in Earth's lower mantle *Science* **317** 1740
[18] Miaja-Avila L *et al* 2015 Laser plasma x-ray source for ultrafast time-resolved x-ray absorption spectroscopy *Struct. Dyn.* **2** 024301
[19] Reich C *et al* 2007 Ultrafast x-ray pulses emitted from a liquid mercury laser target *Opt. Lett.* **32** 427
[20] Zamponi F *et al* 2009 Femtosecond hard x-ray plasma sources with a kilhertz repetition rate *Appl. Phys.* A **96** 51
[21] Smith S J *et al* 2012 Small pitch transition-edge sensors with boradband high spectral resolution for solar physics *J. Low Temp. Phys.* **167** 168
[22] Bergmann U *et al* 1999 Chemical dependence of interatomic x-ray transition energies and intensities—a study of Mn Kβ'' and K$\beta_{2,5}$ spectra *Chem. Phys. Lett.* **302** 119
[23] Ogi Y *et al* 2015 Ultraviolet photochemical reaction of [Fe(III) $(C_2O_4)_3]^{3-}$ in aqueous solutions studied by femtosecond time-resolved x-ray absorption spectroscopy using an x-ray free electron laser *Struct. Dyn.* **2** 034901
[24] Chen J *et al* 2007 Transient structures and kinetics of the ferrioxalate redox reaction studied by time-resolved EXAFS, optical spectroscopy and DFT *J. Phys. Chem.* A **111** 9326
[25] Noroozian O *et al* 2013 High-resolution gamma-ray spectroscopy with a microwave-multiplexed transition-edge sensor array *Appl. Phys. Lett.* **103** 202602
[26] Doriese W B *et al* 2015 *J. Low Temp. Phys.* at press